International Journal of Concrete Structures and Materials
Vol.18, No.3E, pp.145~150, December 2006

Guidelines for Joint Depth Determination and Timing of Contraction Joint Sawcutting for JCP Analyzed with Fracture Mechanics

Sung-Chul Yang[1] and Seung-Ho Hong[2]

(Received September 26, 2005, Accepted December 15, 2006)

Abstract: An experiment with the objective of providing guidelines for joint depth determination and timing of contraction joint sawcutting to avert uncontrolled cement concrete pavement cracking has been conducted. Theoretical analysis and laboratory tests were performed to help in understanding and analyzing the field observation. Using two-dimensional elastic fracture mechanics, the influence of several parameters on crack propagation was delineated by a parametric study, involving initial notch ratio, joint spacing, Young's modulus and thermal expansion coefficient of concrete, temperature gradient, and modulus of subgrade reaction. Bimaterials made of rock plus cement mortar and rock plus polymer mortar were applied to the concrete in a field test section, and they were subjected to fracture tests. These tests have shown that fracture mechanics is a powerful tool not only in judging the quality of the jointed cement concrete pavement but also in providing a criterion for crack propagation and delamination. Based on fracture mechanics, a method is proposed to determine the joint depth, sawcut timing, and spacing of the jointed cement concrete pavement. This method has successfully been applied to a test section in Seohaean expressway. This study also summarizes the research results obtained from a field test for jointed plain concrete pavement, which was also carried out on the Seohaean expressway.

Keywords: fracture mechanics, joint depth, contraction joint, size effect law (SEL), fracture toughness

1. Introduction

The portland cement concrete pavement has been widely used in Korea since 1983, and highway engineers have been concerned with repairing and management of the cement concrete pavement. More than 60 percent of the concrete pavement are composed of jointed plan concrete pavement. The service life of existing concrete pavements is now nearly exhausted, and research on better repair and rehabilitation methods for the pavement as well as on better pavement materials is in a great demand. Therefore, the behavior of concrete pavement system needs to be investigated to develop better repairing methods and their materials.

Concrete pavements are deteriorated due to environmental loading as well as traffic loading. The environmental stresses are ascribed to curling or warping which is caused by thermal stresses or shrinkage stresses.[1]

Moreover, stresses may be induced due to the fraction between the slab and lean concrete. When such induced tensile stresses exceed the concrete tensile strength, a random crack forms at the weakened place. A method to avert this induced uncontrolled crack is to form a contraction joint with a joint interval of six meters prior to the concrete is hardened.

First of all, a preliminary experimental test has been conducted to determine the fracture toughness of the concrete. Then, a theoretical analysis was conducted to determine the optimum saw cutting depths. Using two-dimensional linear elastic fracture mechanics, the influence of several parameters (initial notch ratio, joint spacing, Young's modulus and thermal expansion of concrete, temperature gradient, and modulus of subgrade reaction) on crack propagation was delineated by a parameter study.

2. Mechanical study

2.1 Theory and application of fracture mechanics

The analysis of notched concrete pavement slab by fracture mechanics considers the stresses generated by temperature and shrinkage effects, which are applied as loads. Important material parameters as identified by the size effect law (SEL) [2,5-7] are determined based on notch beam tests. The notch depth is large enough so that the crack will develop quickly and extend to the slab bottom under the applied stress. Through fracture tests, fracture parameters, K_{If} and c_f have been obtained for concrete at different ages. The K_{If} is a critical stress intensity factor for a specimen of infinite dimension (in depth) in which linear elastic fracture mechanics (LEFM) is applied for the analysis. The c_f is the length of process zone for an infinitely large specimen. The application of K_{If} to a concrete slab can not extend to an infinitely large specimen in practice. This is because the nominal strength of an infinite specimen is lower than the nominal strength of a finite

[1] KCI member, Dept. of Architectural Engineering, Hongik University Chungchongram-do 339-701, Korea.
[2] KCI member, Pavement Research Group, Highway & Transportation Technology Institute, Korea Highway Corporation, Gyeonggi-do 445-812, Korea. *E-mail: hsh373@freeway.co.kr*

specimen, which is predicted with LEFM based on K_{If} as the failure criterion.

As in linear mechanics, the superposition principle can be applied to the stress intensity when a specimen or structure is subjected to more than one load. The stress intensity factor due to any load can always be expressed as follows:

$$K_I = \sigma_N \sqrt{\pi a} N(w) \quad (1)$$

Where σ_N is defined as the nominal stress, a is the crack length, and $N(w)$ is a non-nominal function of the ratio, w, of the crack length to the specimen dimension. $N(w)$ is called nominal stress intensity factor. The beam depth (slab thickness h) is usually taken as the dimension d. The nominal stress intensity factor is dependent on the specimen geometry, but it is independent of the specimen size. The nominal stress intensity factor $N(w)$ for simple tension is :

$$N(w) = 1.122 - 0.231w + 10.550w^2 - 21.710w^3 + 30.382w^4 \quad (2)$$

For pure bending[7] :

$$N(w) = 1.122 - 1.40w + 7.33w^2 - 13.08w^3 + 14.0w^4 \quad (3)$$

Note that these two formulas are for the geometry with top and bottom surfaces free from external forces. Fig. 1 shows the tendency for curling and warping due to the temperature gradient and shrinkage.

The finite element analysis in this study showed that replacement of the distributed load on a specimen in simple tension by its resultant concentrated load acting along the specimen centerline did not yield a significant change in the K_I value, particularly when the specimen length was four times the thickness.

2.2 Brief review of size effect law

The size effect law (SEL)[6,7] was generalized by introducing two material fracture parameters, fracture energy G_f and process zone length c_f for an infinitely large specimen. When the specimen is infinitely large, the process zone length can always fully develop with no constraint from the specimen boundary; therefore, c_f is a material constant. In addition, c_f is negligible when the initial crack length, a_o, is sufficiently long so that linear elastic fracture mechanics applies. Additionally, G_f must be a material constant, and in case of the infinity large specimen, SEL can be synthesized as the following.

$$\sigma_N = c_n \left[\frac{\frac{EG_f}{g'(w_o)}}{c_f + \frac{g(w_o)}{g'(w_o)} d} \right]^{1/2} \quad (4)$$

where, E is elastic modulus, $w_o = a_o/d$, and σ_N is the nominal strength of the specimen (or structure) defined as the following.

$$\sigma_N = c_n \frac{P}{bd} \quad (5)$$

in which P in the maximum load, b is the specimen thickness, d is the specimen dimension (i.e., the depth for the beam), and c_n is an arbitrarily defined constant. Then,

$$g(w) = f^2(w) = \pi \alpha c_n^2 N^2(w)$$

where, w is the ratio of the crack length α to the specimen dimension d, and $f(w)$ is the geometry factor for the stress intensity factor K_I in Eq. (1).

For a specimen (or structure) of any geometry and any size, the function $f(w)$ can be obtained by LEFM analysis. Formulas for specimens or structures of much popular geometries have been analyzed and can be found in the manuals. Thus, with EG_f and c_f known, the nominal strength of a structure can be determined by the general SEL equation of (4). It is noted that although $g(w_o)$ and $g'(w_o)$ are calculated based on LEFM, σ_N of a finite specimen (or structure) determined by Eq. (4) should not be based on LEFM but be analyzed by a nonlinear model, i.e., SEL. For an infinity large specimen, only LEFM is valid, and, with respect to the LEFM analysis, the critical stress intensity factor K_{If} for an infinity large specimen and EG_f are subject to a plane stress relation to be explained in section 3.2.

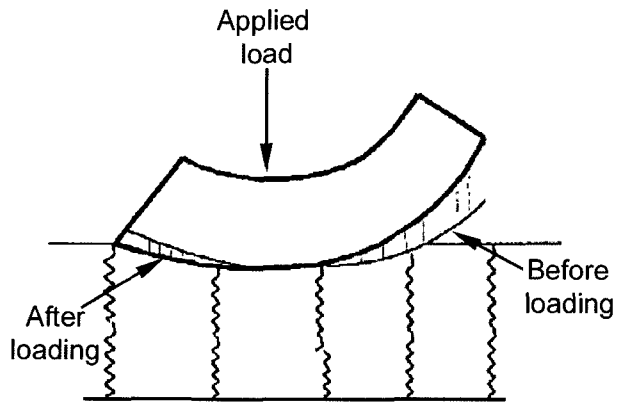

Fig. 1 Curling due to temperature gradient.

3. Results and discussions

3.1 Measurement of fracture toughness

Fracture tests were conducted to determine the K_{If} values using the generalized size effect law. Fracture test specimens of the mix were of eccentric compression prisms. These prisms have the same shape and the same size but different notches. The coarse aggregate was of maximum size of 32 mm, and siliceous sand was used as the fine aggregate. Table 1 gives the mix proportions based an 1 m^3 of Type I cement. This mix design is based on the design that is commonly used for concrete pavements constructed

Table 1 Mix proportions used in field test section.

Slump (mm)	Air content (%)	W/C (%)	S/A (%)	Unit weight					
				Water (kg)	Cement (kg)	Fine aggregate (kg)	Coarse aggregate(kg)		A.E Admixture (kg)
							32 mm	19 mm	
40	4.5	43	30	147	342	688	635	518	0.684

in Korea with slip-formed paving technology, of which the slump ranges from 25.4 mm to 50.8 mm (1 to 2 in.).

A series tests for the cast specimens were conducted in four batches at 1 day, 7 days, 14 days, and 28 days age (one batch per age). Each fracture toughness at 2, 7, 15, and 28 days was calculated from a linear regression by using the generalized size effect law, and the result is shown in Fig. 2. The fracture toughness at 2 days was 0.55 $MPa\sqrt{m}$. The toughness increased fast within 7 days, and it reached 1.09 $MPa\sqrt{m}$ at 20 days.

3.2 2-D Plane stress analysis with Winkler foundation

A classical plate theory is generally accepted for the analysis of thin plates specifically in the area such as plane stress or plane strain elasticity to simulate curling or warping stresses due to thermal or shrinkage change. In this analysis, because of the symmetry, only a half of the pavement system in Fig. 3 was carefully meshed to reduce computation errors. The pavement depth was 300 mm, and pavement length ranged variably from 5.0 to 7.0 meters.

All the finite elements are of 8-node isoparametric elements. The elements around the crack tip are generalized by collapsing

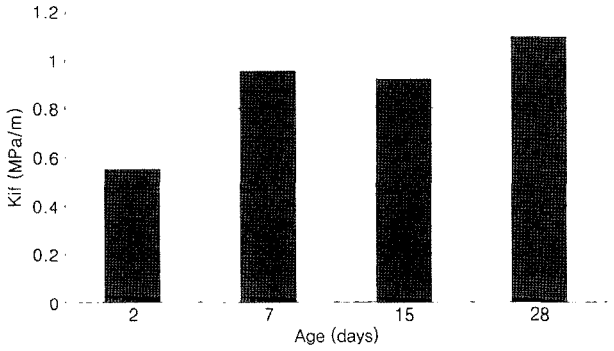

Fig. 2 Fracture toughness with concrete age.

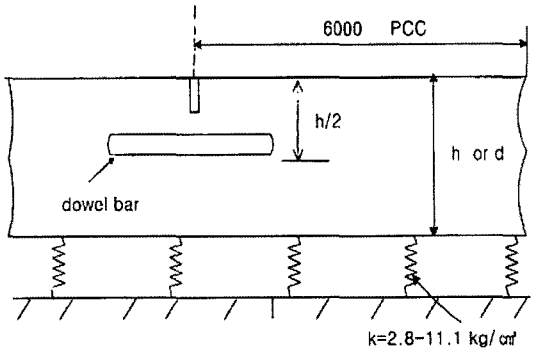

Fig. 3 Layout of joint concrete pavement.

Table 2 Fracture toughness with concrete age.

Age (day)	$K_{If}(MPa\sqrt{m})$	c_f(mm)	R^2
2	0.55	3.7	0.81
7	0.95	3.3	0.91
15	0.92	7.3	0.90
28	1.09	7.8	0.93

one side of the element, and all the mid-side nodes along with the crack tip are moved to the quarter point to generate a stress singularity at the crack tip B. All the nodes on AB are restrained in both x-direction, and the node at B is restrained in both x-direction and y-direction.

All liquid foundation is incorporated for the analysis in this study. To simulate a partial contact without initial gaps of slab-subgrade contact, the springs are to be cut when gaps form at the exterior springs if the slab is curled up as shown in Fig. 1. In order to study the significance of various parameters, the J-integral value, which is an energy requirement for the growth of the crack, was calculated around the crack tip area. One variable at a time was changed while keeping the rest of the variables of Table 3 constant.

The variables of this study are slab thickness, slab length, concrete properties (such as Young's modulus, and coefficient of thermal expansion), thermal gradient through the thickness of concrete slab, and modulus of subgrade reaction.

3.2.1 Thermal gradient (ΔT)

As shown in Fig. 4, the stress intensity factor increases with increased thermal gradients as well as increased initial notch depths. Fig. 4 shows the K_I values for the temperature difference of 11.1°C (20°F), 10.7°C (30°F), 22.2°C (40°F), and 26.9°C (50°F) between the slab top and bottom subjected to induced stresses. Fig. 4 also gives the K_I values with different notch (sawcut) depths

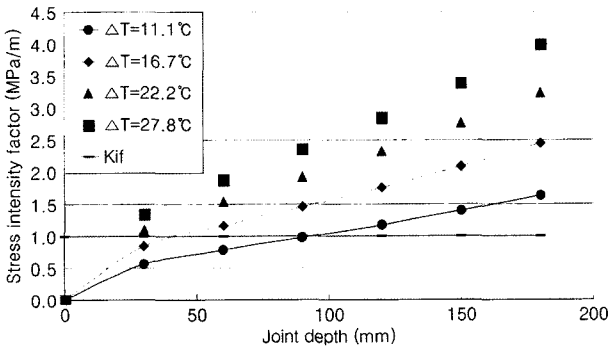

Fig. 4 Stress intensity factor vs joint depth with ΔT.

Table 3 Input data used in parametric analysis.

Variables	Symbol	Unit	Values
Slab thickness	h	mm	305
Slab length	L	m	5.1, 6.1, 7.1
Young's modulus of concrete	E	N/mm^3	2.1×10^4, 2.7×10^4, 3.4×10^4
Poisson's ratio of concrete	ν	-	0.15
Thermal expansion coefficient of concrete	αT	μ/°C	9.0, 11.3, 13.5
Temperature gradient	ΔT	°C	27.8, 22, 20, 16.7, 11.1
Modulus of subgrade reaction	k	N/mm^3	2.7×10^{-2}, 10.8×10^{-2}

under temperature stresses. When the stress intensity factor, K_{If}, is equal to 0.55 $MPa\sqrt{m}$ experimental value at an age of 2 days), a sawcut depth of 25 mm is enough if the temperature difference is not more than 11.1°C (20°F).

Noting the change in stress intensity in comparison to the fracture toughness for a given climate condition, one can develop a sense for the appropriate saw-cut timing to control cracking at the saw-cut notches. Similar to the stress intensity factor, the crack mouth opening displacement (CMOD) in Fig. 5 increases with increased thermal gradient as well as saw cut depths.

3.2.2 Young's modulus and thermal expansion coefficient

Many researchers have reported that Young's modulus of concrete increases with age and vise versa for the thermal expansion coefficient. As Figs. 6 and 7 show, the K_I values vary almost linearly with thermal expansion coefficient and Young's modulus of concrete, respectively. From this relation, it can be inferred that the coarse aggregates is important especially in mix proportioning because it has a great influence on the values of Young's modulus and thermal expansion coefficient. To investigate the behavior of the concrete at an early age, an analysis was carried out with input data of $L = 6.1$ m, $E = 1.4 \times 10^5$ kg/m^2, $\Delta T = 16.7$°C, $K = 2.8$ kg/m^3, $\alpha T = 13.5$ μ/°C, and $w = 0.3$. A solid circle denotes the K_I value for this case. The analysis revealed that a crack is easily formed from the concrete slab, of which property is still young at an early age.

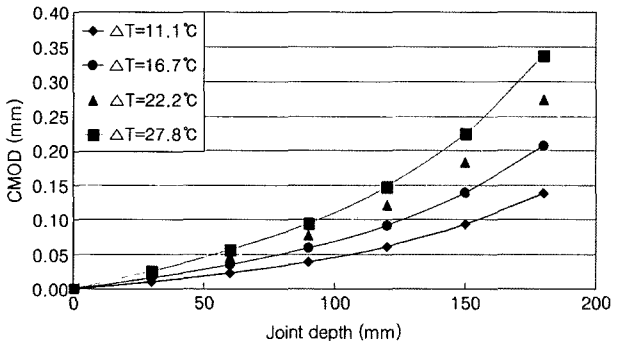

Fig. 5 CMOD vs joint depth with ΔT.

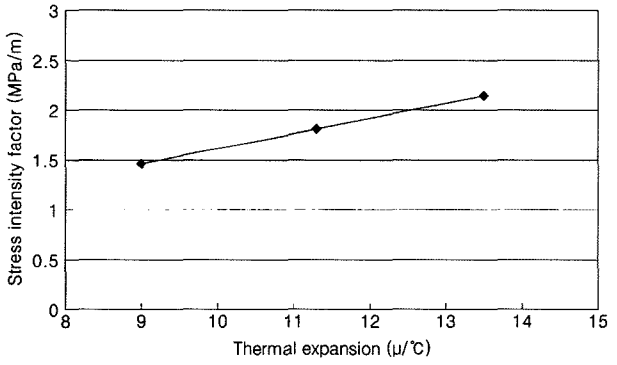

Fig. 6 Stress intensity factor vs thermal expansion coefficient of concrete.

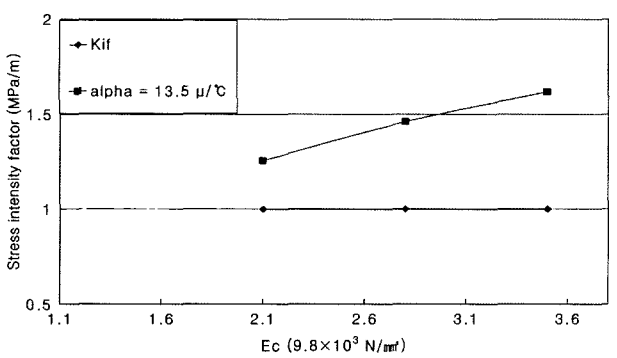

Fig. 7 Stress intensity factor vs Young's modulus of concrete.

3.2.3 Longitudinal slab length

Three different slab lengths were considered in a numerical analysis to investigate their influence on the K_I values. As Fig. 8 shows, some erroneous results were obtained. The K_I has a maximum value when the slab length is 6.1 m over a closed interval (from 5.1 to 7.1 m) of a concave function. It is contradictory to the common concept that a longer slab is more vulnerable to cracking. Further analysis is needed to investigate this behavior.

3.2.4 Modulus of subgrade reaction

An increase in the modulus of subgrade reaction does not seem to change the K_I value much as shown in Fig. 9, but the K_I value decreases with increasing modulus of the subgrade reaction. This phenomenon was also observed at test section constructed of different subbase types at Rothsay, MN in 1970.[3]

It is concluded from the field observation that the trend toward greater saw cut depths may be due to the trend toward the use of treated subbase. As Fig. 9 shows a stiffer subbase type needs a greater saw cut depth.

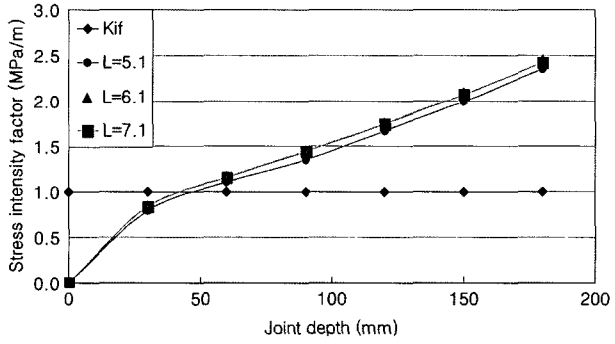

Fig. 8 Stress intensity factor vs joint depth with slab length.

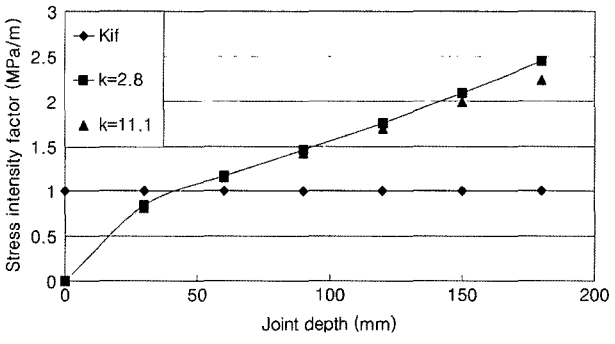

Fig. 9 Stress intensity factor vs joint depth with modulus of subgrade reaction.

3.3 Field observation of crack control

The factors, that affect the behavior of concrete pavements as those related to joint formation and crack control, were monitored in a field study performed at test sections of 300 mm jointed plain concrete pavement placed on a 150 mm lean concrete pavement at Seohaean expressway. Different sawcut depths of 60 mm (denoted as *d/5*), 75 mm (denoted as *d/4*), and 100 mm (denoted as *d/3*) were experimented at the test section. The *d/4* test section was paved from 12 : 30 ~ 15 : 30 PM on August 26. The *d/3* test section was paved from 07 : 40 to 10 : 10 AM the following day while the *d/5* test section was continuously paved from 10 : 10 AM to 13 : 20 PM.

The joint in the test section pavement was sawcut by the conventional method. Early-aged sawcut operations generally started 6 to 11.5 hours after the placement of concrete. The experienced contractor determined sawcut timing by visual inspection and walking on the slab. The *d/4* test section was sawcut about 7 hours after the placement of the concrete. Meanwhile, the *d/3* test section and *d/5* test section were sawcut about 8~11.5 hours, and 6~8 hours after the placement of the concrete, respectively.

It is interesting to note how different sawcut depths affect the fracture properties and crack development of concrete pavement as shown in Fig. 10. Cracking at every sawcut tip occurred overnight where the test section was sawcut 100 mm deep (*d/3* test section). On the contrary, 28 percent and 71 percent of the sawcut have cracked overnight at the *d/4* test section and *d/5* test section, respectively. However, both the two sections (*d/4* and *d/5*) cracked at every sawcut tips eventually after a month. Thus, it is concluded from the field study that cracking at the sawcut tip is affected more strongly by sawcut timing rather than sawcut depth. Moreover, the equivalent age concept as another indication of so-called maturity could be used to determine the sawcut timing.

3.4 Gauge installation and measurement

Electronics sensors were installed at predetermined locations in the test sections to measure the pavement performance.

(1) Crack mouth opening displacement at sawcut tip was measured by crack gauges located at the transverse joint. Gauges were located near the slab edges as shown in Fig. 11.

(2) Gap between the slab and lean concrete due to curling or warping was measured by crack gages located in vertical housing of the pavement. Sensors as depicted in Fig. 12 were installed under wheel-paths and transverse joint at mid-slab location. Crack width varies with temperature; cracks are wider in cold weather, when the concrete slabs have contracted, than in hot weather, when the individual concrete slabs have expanded. Fig. 13 shows the CMOD measurement with time.

A crack gauge mounted on the surface of slab 28 (S28) showed a minimum displacement CMOD of −0.0582 mm and a maximum CMOD of 0.4342 mm. The CMOD value of slab 29 (S29) had a

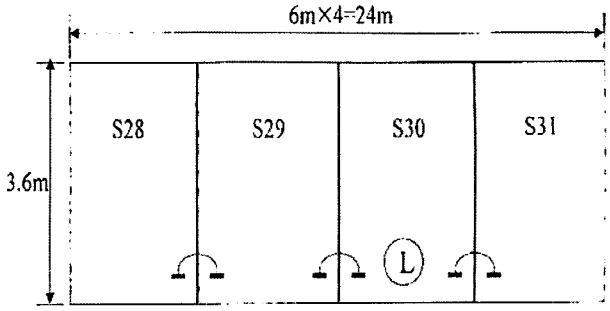

Fig. 11 Layout of test section.

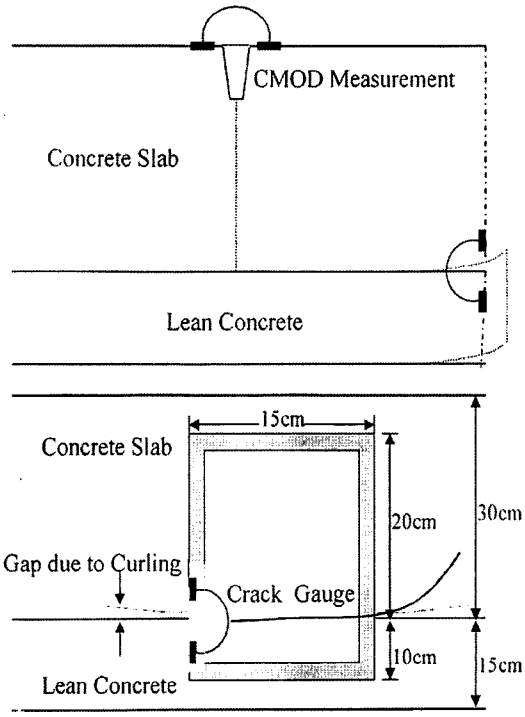

Fig. 12 Installation of crack gauge.

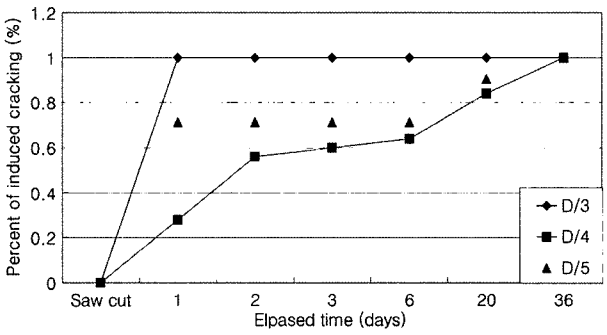

Fig. 10 Percentage of induced crack from different test section.

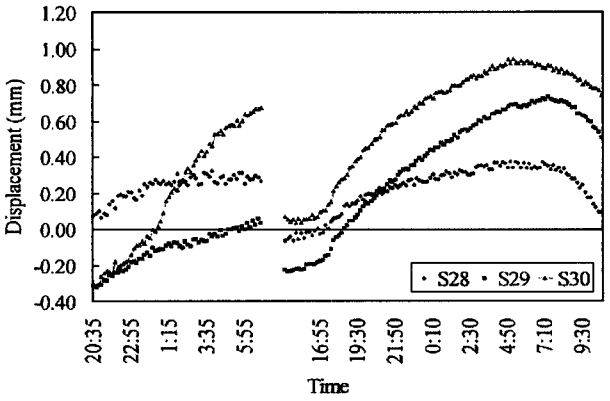

Fig. 13 Measured displacement at crack tip with time.

minimum value of −0.3108 mm and a maximum value of 0.7390 mm while the CMOD value of slab 30 (S30) exhibited a minimum of −0.3098 mm and a maximum of 0.9479 mm.

It was well summarized by Suh[8] that factors affecting the crack width are the time of crack occurrence, crack spacing, and slab temperature among others. It was reported in a field study that the cracks, which had occurred during the first three days after the construction, were significantly wider than those that occurred later. This was explained by the residual shrinkage of the later crack, consequently resulting in the greater crack width at the earlier age. As mentioned previously in the two-dimensional plane stress analysis, the effect of crack spacing on the crack width was not significant. This was confirmed by his field observation.

A gap between the slab and lean concrete (or foundation) occurs due to the temperature differential between the top and the bottom of the pavement slab. Thus, the gap varies with time of the day. Fig. 14 shows the gap displacement measurement with time of the day. One can notice from the figure that gaps are wider in cold weather, when the concrete slabs have contracted, than in hot weather, when the individual concrete slabs have expanded.

A crack gauge mounted vertically along the sections of the slab and lean concrete in the *d/3* test section had a minimum displacement of −0.2973 mm at 14 : 00PM and a maximum displacement of 0.1851 mm around 06 : 00AM. The ambient temperature ranged from 22°C to 28°C during the day of the measurement.

4. Conclusions

A study with the objective of providing guidelines for timing of contraction joint sawcutting and joint depth determination has been conducted to avert uncontrolled cement concrete pavement cracking. Theoretical analysis and laboratory tests were performed to help in understanding and analyzing the field observation. This paper also summarized the research results obtained from a field test for jointed plain concrete pavement, which was carried out on the Seohaean expressway.

1) Fracture tests from eccentric compression prism were conducted to determine the K_{If} values using the generalized size effect law. The fracture toughness at the second day was 0.55 $MPa\sqrt{m}$. The toughness increased fast within seven days, and it reached 1.09 $MPa\sqrt{m}$ at 28 days.

2) Using two-dimensional linear elastic fracture mechanics, the influence of several parameters on crack propagation was delineated by a parameter study, involving initial notch ratio, joint spacing, Young's modulus, thermal expansion of concrete, temperature gradient, and modulus of subgrade reaction.

3) The K_I had a maximum value when the slab length was 6.1 m at a closed interval (from 5.1 to 7.1 m) of a concave function. This is contradictory to the common concept that a longer slab is more vulnerable to cracking. Further analysis is needed to investigate this seemingly erroneous behavior.

4) An increase in the modulus of subgrade reaction does not seem to change the K_I value much as shown in Fig. 9, but the K_I value decreases with increasing modulus of the subgrade reaction. Thus, a stiffer subbase type needs a greater saw cut depth.

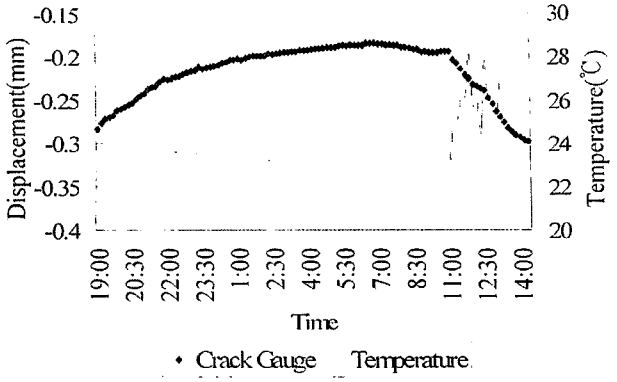

Fig. 14 Gap displacement between slab and lean concrete.

5) Crack width varied with temperature and time. The CMOD value at slab 30 (S30) had a minimum of −0.3098 mm measured at about 14 : 00PM and a maximum of 0.9479 mm measured at about 06 : 00AM.

6) A gap between the slab and lean concrete (or foundation) varied with time. A crack gauge mounted vertically along the sections of the slab and lean concrete had a minimum displacement of −0.2973 mm at 14 : 00PM and a maximum displacement of 0.1851 mm around 06 : 00AM. The ambient temperature ranged from 22°C to 28°C during the day of the measurement.

References

1. Haung, Y. H., *Pavement Analysis and Design*, Prentice Hall, New Jersey, 1993, 775pp.

2. Tang, T., Zollinger, D. G., and McCulloug, B. F., *Field Tests and Analyses of Concrete Pavements in Texarkana and La Porte*, Texas, TTI Research Report 1244-7, Texas A & M University System, College Station, Texas, 1994.

3. Okamoto, P. A., et al., *Guidelines for Timming Contraction Joint Sawing and Earliest Loading for Concrete Pavements Volume I*, FHWA Report RD-91-079, Washington, DC, 1994.

4. Anderson, T. L., *Fracture Mechanics 2nd Edition*, CRC, 1995. 688pp.

5. Karihaloo, B. L., *Fracture Mechanics & Structural Concrete*, Longman, 1995. 400pp.

6. Bazant, Z. P. and Kazemi, M. T., "Determination of Fracture Energy, Process Zone Length and Brittleness Number from Size Effect, with Application to Rock and Concrete", *International Journal of Fracture*, Vol.44, No.2, 1990, pp.111~131.

7. Tang, T., Bazant, Z. P., Yang, S., and Zollinger, D., "Variable-Notch One-Size Test Method for Fracture Energy and Process Zone Length," *Journal of Engineering Fracture Mechanics*, Vol.55, No.3, 1996, pp.383~404.

8. Suh, Y. C., *Early-Age Behavior of CRCP and Calibration of Failur Prediction Model in CRCP-7*, Ph.D. Thesis, The University of Texas at Austin, 1991.